Current Biology 20, 643–648, April 13, 2010 ©2010 Elsevier Ltd All rights reserved DOI 10.1016/j.cub.2010.01.060

Report

Inactivation of Both *foxo* and *reaper* Promotes Long-Term Adult Neurogenesis in *Drosophila*

Sarah E. Siegrist,[1] Najm S. Haque,[1] Chun-Hong Chen,[2,3] Bruce A. Hay,[3] and Iswar K. Hariharan[1,*]

[1]Department of Molecular and Cell Biology, University of California, Berkeley, Berkeley, CA 94720-3200, USA

[2]Division of Molecular and Genomic Medicine, National Health Research Institutes, Zhunan Town, Miaoli County 350, Taiwan

[3]Biochemistry and Molecular Biophysics, California Institute of Technology, Pasadena, CA 91125, USA

Summary

Adult neurogenesis occurs in specific locations in the brains of many animals, including some insects [1–3], and relies on mitotic neural stem cells. In mammals, the regenerative capacity of most of the adult nervous system is extremely limited, possibly because of the absence of neural stem cells. Here we show that the absence of adult neurogenesis in *Drosophila* results from the elimination of neural stem cells (neuroblasts) during development. Prior to their elimination, their growth and proliferation slows because of decreased insulin/PI3 kinase signaling, resulting in nuclear localization of Foxo. These small neuroblasts are typically eliminated by caspase-dependent cell death, and not exclusively by terminal differentiation as has been proposed [4]. Eliminating Foxo, together with inhibition of *reaper* family proapoptotic genes, promotes long-term survival of neuroblasts and sustains neurogenesis in the adult mushroom body (mb), the center for learning and memory in *Drosophila*. Foxo likely activates autophagic cell death, because simultaneous inhibition of *ATG1* (autophagy-specific gene 1) and apoptosis also promotes long-term mb neuroblast survival. mb neurons generated in adults incorporate into the existing mb neuropil, suggesting that their identity and neuronal pathfinding cues are both intact. Thus, inhibition of the pathways that normally function to eliminate neural stem cells during development enables adult neurogenesis.

Results and Discussion

The *Drosophila* brain provides an excellent model system in which to investigate how neurogenesis becomes progressively restricted because neurons are generated only during development and not in adulthood [5–7]. All neurons within the central brain are generated from the asymmetric cell divisions of neural stem cells known as neuroblasts [8–10]. Neuroblasts are large in size and mitotically active, likely dividing every 1–2 hr during later larval development [6, 11]. Because central brain neuroblasts divide only asymmetrically and never symmetrically, their numbers remain constant. Therefore, they can be followed unambiguously over time with neuroblast-specific molecular markers [12]. Because neurogenesis at all stages of development is characterized by the presence of neuroblasts, we first examined whether adult *Drosophila* brains have neuroblasts. We detected no cells displaying the molecular signature of neuroblasts in young (3–5 days posteclosion) adult brains, i.e., (1) expression of Deadpan (Dpn), a neuroblast transcription factor, (2) expression of Miranda (Mira), a cargo carrier of cell fate determinants, and (3) nuclear exclusion of Prospero (Pros) (n > 10 adult brains). Consistent with previous studies [5–7], we also found no evidence for cell proliferation in these young adult brains either via mosaic analysis with a repressible cell marker (MARCM) [13], a genetic technique that positively marks cells only after cell division, or by administering BrdU, a thymidine analog. Therefore, adult neurogenesis is likely absent because no actively dividing neuroblasts are present in the adult *Drosophila* brain.

Reduction in Neuroblast Growth Precedes Neuroblast Disappearance

To understand why adult neuroblasts are not present, we examined brains at earlier developmental stages, when neuroblasts are still present. Using an antibody to Dpn and an E2F-responsive GFP reporter (*pcna:eGFP*) [14] (Figures 1A and 1D), we identified 100 ± 2.73 (mean ± standard deviation [SD], n = 8 brain lobes) large neuroblasts within the central brain of each brain lobe in mid L3 larvae (96 hr after larval hatching) during the height of neurogenesis (Figures 1B and 1C). This is consistent with previous reports [6, 12]. Approximately 30 hr later, at 5 hr after puparium formation (APF), neuroblast number remained unchanged but neuroblast cell size and mitotic activity were reduced (Figures 1B and 1C), suggesting that neuroblast growth and division rates were changing. By 30 hr APF, only a few small neuroblasts remained other than the mushroom body (mb) neuroblasts (Figure 1B; data not shown) (see below). This coincided with a complete shut down in cell proliferation, as assessed by the lack of *pcna:eGFP*-expressing cells (compare Figure 1A to Figure 1D). Thus, during early pupal stages, most central brain neuroblasts decrease their rates of growth and proliferation, raising the possibility that these changes trigger neuroblast disappearance and terminate neurogenesis.

Of all the neuroblasts in the central brain, only the mb neuroblasts remain midway through pupal development [6, 15] and are all located on the dorsal surface of the central brain, superficial to the mb calyx (Figures 1D and 1E). At 15 hr APF, mb neuroblasts can be positively identified among the remaining central brain neuroblasts (Figure 1A), solely based on their size (average diameter = 11.6 μm, SD ± 0.93, n = 48). They remained large and mitotically active, similar to larval neuroblasts, until 72 hr APF (Figures 1B, 1C, 1E, and 1F). After this, we observed a significant decrease in mb neuroblast cell size, followed 6 hr later by a strong reduction in their mitotic activity (Figures 1E and 1F). By 96 hr APF, approximately 10 hr before adult eclosion, essentially no mb neuroblasts were detected (Figure 1E). Therefore, all neuroblasts, including the late-persisting mb neuroblasts, experience a reduction in growth prior to their disappearance, suggesting that a common lineage-independent mechanism links a decrease in growth with neuroblast disappearance.

*Correspondence: ikh@berkeley.edu

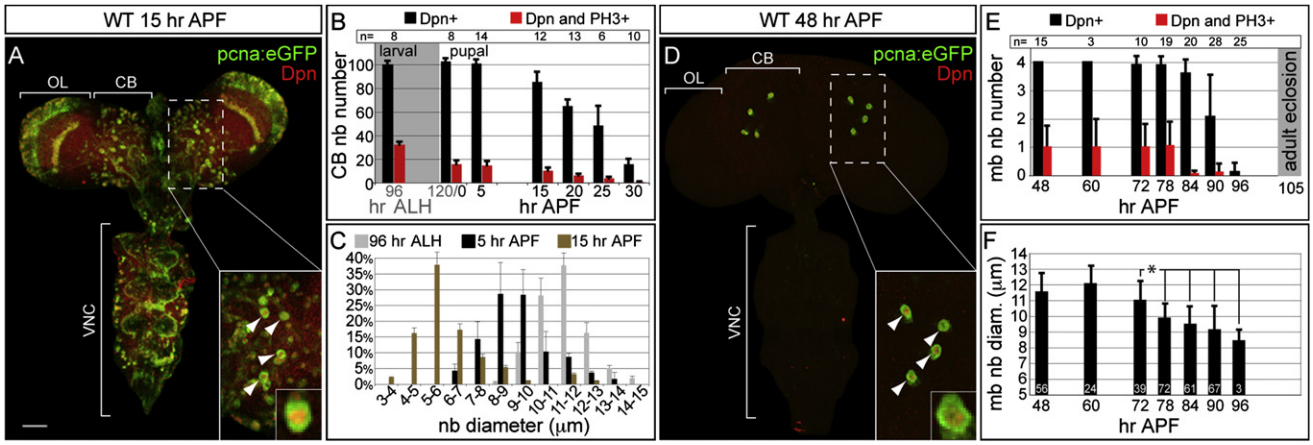

Figure 1. Neuroblast Growth Becomes Restricted during Pupal Development

(A and D) Z projection of the brain (optic lobe [OL] and central brain [CB]) and ventral nerve cord (VNC) from wild-type (WT) animals (pcna:eGFP transgenic) at 15 hr (A) or 48 hr (D) after pupal formation (APF). Neuroblasts express Deadpan (Dpn, red) and the E2F reporter pcna:eGFP (GFP, green). Scale bar in (A) equals 50 μm.

(B and E) Quantitation of CB (including the mushroom body [mb] neuroblasts [nbs]) (B) and mb (E) neuroblast number and number of mitotic neuroblasts based on PH3 (phosphohistone H3) per brain lobe over time. n denotes number of brain lobes scored per time point.

(C) Distribution of CB neuroblast cell size over time. The average diameter of all CB neuroblasts from three brain lobes (three animals) was measured for each of three time points.

(D) Only the four mb neuroblasts located on the dorsal CB surface persist late (arrowheads in A and D). Dotted box denotes area of CB magnified in larger inset with one of the four mb neuroblasts in small inset.

(F) Quantitation of the average diameter (diam.) of mb neuroblasts over time. Numbers of mb neuroblasts measured for each time point are shown as white numbers in black columns. *$p < 0.001$. Columns represent mean ± standard deviation (SD) in this and all subsequent figures. ALH denotes after larval hatching.

Mushroom Body Neuroblasts Are Eliminated via Reaper-Dependent Cell Death

A recent study [4] concluded that the most likely explanation for neuroblast disappearance within the central brain is terminal differentiation, which requires Pros to localize to the neuroblast nucleus after the final cell division. Therefore, we first examined mb neuroblasts for evidence of nuclear Pros at the time that best approximates when the final cell divisions of these neuroblasts occur (Figure 1E). Although nuclear localization of Pros could be transient and hence difficult to observe, we and others [15] found no evidence of Pros in the nuclei of mb neuroblasts at 84 or 90 hr APF (see Figures S1C and S1D available online). This suggests that a mechanism other than terminal differentiation could account for mb neuroblast disappearance. Because neuroblasts located in the abdominal segments of the ventral nerve cord are eliminated by apoptosis [16, 17], we next tested whether central brain neuroblasts, including the mb neuroblasts, undergo cell death. Indeed, at 25 and 90 hr APF, when either central brain or mb neuroblast number was dramatically declining, we observed neuroblasts displaying characteristics of dying cells, i.e., activated caspase, fragmented DNA, and no nuclear envelope (Figures 2A–2C; Figures S1A and S1B). Taken together, these results suggest that at least some central brain neuroblasts, including the mb neuroblasts, are eliminated by apoptosis and not differentiation.

If this were the case, then central brain neuroblasts would persist in animals with reduced levels of the Reaper family of proapoptotic regulators. We examined brains from animals transheterozygous for two overlapping deletions, *Df(3L)H99* and *XR38* [17]. These animals, hereafter referred to as *rpr* mutants, were homozygous null for *reaper* (*rpr*) and heterozygous for *hid*, *grim*, and *sickle*, all four of which are proapoptotic genes [18]. At 30 hr APF, *rpr* mutant brains had more neuroblasts than wild-type controls (Figure 2G). This was not due to the initial specification of extra neuroblasts or symmetric neuroblast cell divisions, because *rpr* mutant larval brains have a normal number of large, Dpn-expressing neuroblasts at earlier stages (data not shown). Central brain neuroblasts aberrantly persisted even at 48 hr APF (Figures 2D, 2E, and 2G), but their numbers were considerably reduced. We also observed transient persistence of mb neuroblasts in brains of young adult *rpr* mutants (Figures 2H, 2I, and 2K; Movies S1 and S2). This delay in neuroblast disappearance could be due to residual proapoptotic activity in *rpr* mutants. Therefore, we used MARCM [13] to generate neuroblasts that are homozygous null for *reaper*, *hid*, and *grim* (*H99*). We observed Dpn-expressing cells in *H99* mutant mb neuroblast clones only (Figure S1E) in brains of young (3–5 days posteclosion) adult animals ($n > 40$ central brain neuroblast clones scored), suggesting that neuroblasts are still eliminated despite removal of additional proapoptotic genes. Unfortunately, the low frequency of *H99* mutant mb neuroblast clones precluded the use of this method for a detailed study of the fate of persisting adult mb neuroblasts at all stages. Therefore, we engineered a transgene, *UAS-RHG* microRNA (miRNA), which generates miRNAs that simultaneously inhibit *reaper*, *hid*, and *grim*, and targeted expression of this transgene to neuroblasts with *worniuGAL4* (hereafter referred to as *RHG* miRNA) (Figure S2). In the brains of young *RHG* miRNA adults, the only neuroblasts observed were mb neuroblasts, whose persistence, again, was only transient (Figures 2J and 2K). Similar results were observed following *worniuGAL4*-induced expression of baculovirus p35, an inhibitor of active caspases (Figures 2F, 2G, and 2K). Thus, Reaper family proteins and caspase activation are necessary for the proper timing of

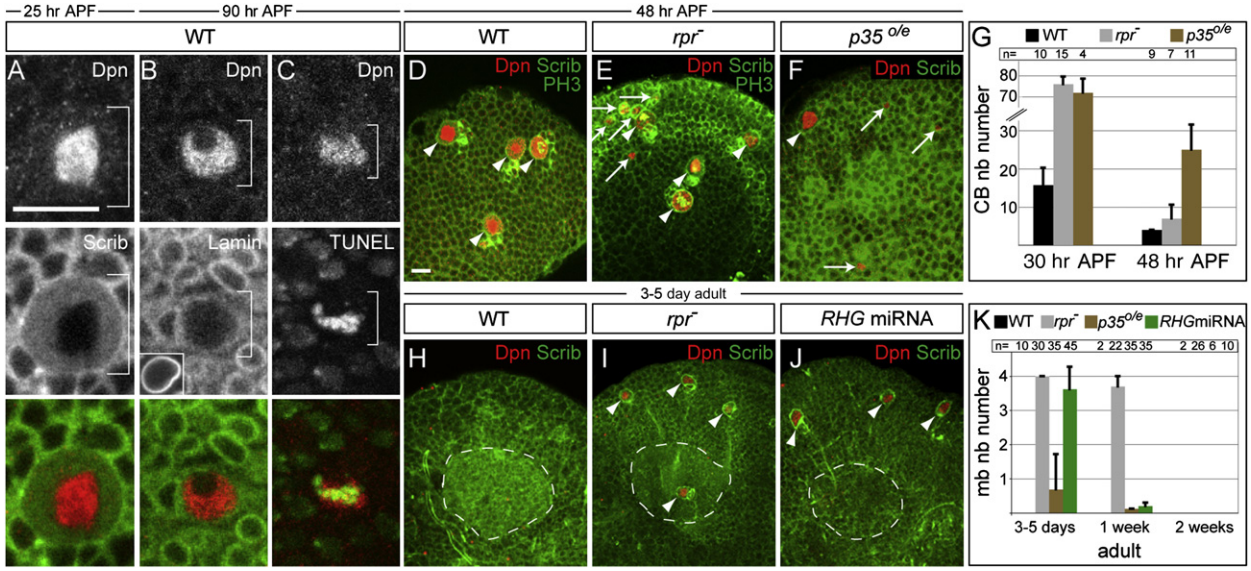

Figure 2. Reaper Family Proapoptotic Regulators and Caspase Activation Are Required for the Proper Timing of Neuroblast Cell Death

(A–C) Wild-type (WT) mb neuroblasts undergo cell death (B and C). Developmental time and genotype are listed above panels, and markers are listed within panels in this and all subsequent figures. Top two rows show single channel images with colored overlay in bottom row showing colocalization of cell death and neuroblast markers (B and C). mb neuroblast (indicated by brackets) are shown at early pupal stages (A) and prior to their death (B and C). DNA fragmentation (C, TUNEL) and nuclear envelope breakdown, as indicated by an absence of Lamin staining (B), are hallmarks of cell death (compare with Lamin staining of an mb neuroblast with an intact nuclear envelope, B, inset).

(D–F and H–J) Z projections of the dorsal, anterior CB surface. Aberrantly persisting neuroblasts are marked with white arrows, and mb neuroblasts are marked with arrowheads. In *rpr*$^{-}$ and *RHG* miRNA adults, the aberrantly persisting neuroblasts are the mb neuroblasts. Only one of the four mb neuroblasts is shown in (F).

(H–J) The mb calyx is outlined by the white dash.

(G and K) Quantitation of Dpn-expressing CB or mb neuroblast number per brain lobe over time. n denotes number of brain lobes scored at each time point. *worniuGAL4* is used to induce upstream activating sequence (UAS) transgene expression (F, G, J, and K).

Scale bars in (A) and (D) equal 10 μm. See also Figures S1 and S2.

neuroblast removal. In their absence, neuroblast elimination is only delayed, suggesting that an alternative caspase-independent pathway compensates to ensure neuroblast removal. Interestingly, neuroblasts persisted longer in *rpr* mutant adults than in those expressing *RHG* miRNA, which could be due to downregulation of *worniuGAL4* (Figures S1F and S1G). This may indicate that neuroblasts rescued from an apoptotic fate have decreased transcription of neuroblast-specific genes, which may contribute to their disappearance via an alternative mechanism.

Cell Death-Inhibited Mushroom Body Neuroblasts Have Impaired Growth

Next we examined the fate of the persisting mb neuroblasts in the brains of young (3–5 days posteclosion) *rpr* mutant adults. Persisting mb neuroblasts expressed both *pcna:eGFP* and Mira, showed an enrichment of membrane-bound Scribble (Scrib), and excluded Pros from the nucleus, all indicators of proper neuroblast cell fate (Figures S3A, S3B, and S3D). They also expressed the mb-specific marker, Eyeless (Ey), and failed to express Elav or Repo, two markers characteristic of differentiated neuronal and glial cell fates, respectively (Figures S3C and S3E). However, the persisting adult mb neuroblasts were only half of the size of mb neuroblasts present during earlier stages of development (Figures 3A and 3D; quantified in Figure 4A), and they divided slowly (Figures S3F–S3H), generating very few new adult mb neurons (Figures S3I–S3L). Thus, growth of persisting mb neuroblasts may be impaired, which could contribute to neuroblast elimination via a caspase-independent pathway.

Consistent with this possibility, we observed that changes in the subcellular localization of the transcription factor Foxo correlate with changes in mb neuroblast cell size. Foxo was mostly cytoplasmic in wild-type larval neuroblasts at a time when growth rates are high, consistent with elevated insulin/PI3 kinase signaling [19, 20] (Figures 3A and 3E). However, more Foxo was observed in the nucleus in pupal mb neuroblasts at 72 hr APF (Figures 3C and 3E), when neuroblast size decreases (Figures 1E and 1F), suggesting that insulin/PI3K signaling is reduced in these cells. This increase in nuclear Foxo was equivalent to that observed in larval neuroblasts that expressed a dominant-negative insulin receptor (InR DN) transgene (Figures 3B and 3E). Levels of nuclear Foxo were even further elevated in the persisting mb neuroblasts observed in *rpr* mutant adults (Figures 3D and 3E). Thus, the Reaper-independent pathway that eliminates neuroblasts may be activated by a reduction in insulin/PI3 kinase signaling.

Next we asked whether insulin/PI3 kinase activity regulates mb neuroblast cell death. We overexpressed Dp60 [21] in mb neuroblasts to inhibit PI3 kinase and observed that mb neuroblasts undergo premature cell death (Figures 3F and 3G). Conversely, mb neuroblasts persist slightly longer in *foxo* mutants or when they express a constitutively active insulin receptor transgene, but are still eliminated via cell death (Figures 3F and 3H; data not shown). Therefore, levels of insulin/PI3 kinase signaling regulate timing of caspase-induced cell death of mb neuroblasts.

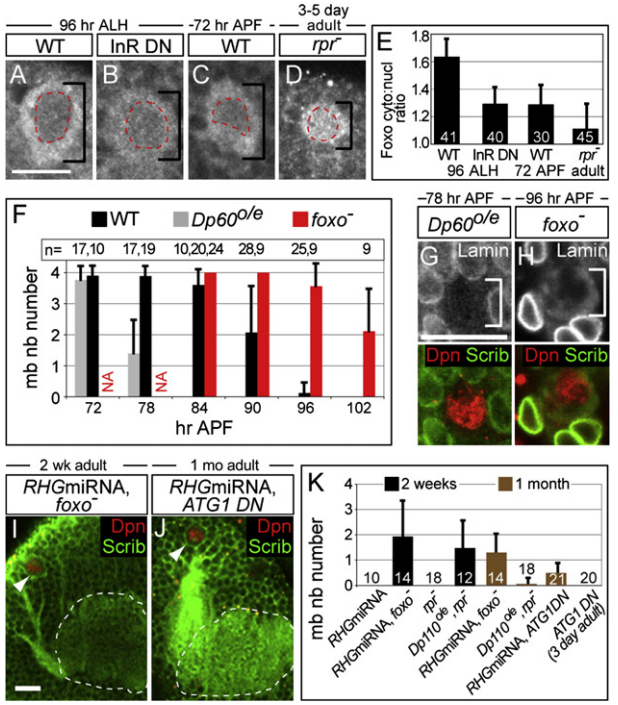

Figure 3. Increased Levels of Nuclear Foxo Restrict Long-Term Survival of mb Neuroblasts

(A–D) Subcellular localization of Foxo in neuroblasts. All neuroblasts were imaged under same settings for direct comparison. Neuroblasts are marked with black brackets, and their nuclei are outlined in red.

(E) Quantitation of the ratio of cytoplasmic to nuclear Foxo protein, based on fluorescence pixel intensities. White numbers in black columns denote number of neuroblasts scored for each genotype at the indicated time.

(F) Quantitation of mb neuroblast number over time (mean ± SD). Dp60 overexpression (o/e) inhibits PI3 kinase signaling, leading to premature mb neuroblast cell death (F and G), whereas *foxo* mutant mb neuroblasts delay death (F and H). n denotes number of brain lobes scored for each genotype at each time point (F).

(G and H) Dying mb neuroblasts lack a nuclear envelope. Compare Lamin staining with inset in Figure 2B. Top panels are single image, and bottom row is overlay.

(I and J) Z projections of the dorsal brain surface showing persisting adult mb neuroblasts (arrowheads) near the mb calyx (white outline).

(K) Quantitation of mb neuroblast number over time. Numbers in columns denote number of brain lobes scored for each genotype at the indicated time. *worniuGAL4* is used to induce UAS transgene expression (B, E–G, and I–K).

Scale bars in (A), (G), and (I) equal 10 μm. See also Figure S3.

Foxo Restricts Growth and Survival of Apoptosis-Inhibited Mushroom Body Neuroblasts

To examine the consequences of maintaining insulin/PI3 kinase signaling in mb neuroblasts with decreased function of Reaper family proteins, we either removed *foxo* function [19] or overexpressed *Dp110*, the catalytic subunit of PI3 kinase [22] (*Dp110$^{o/e}$*). We observed Dpn-expressing mb neuroblasts in 2-week-old and even in 1-month-old *RHG* miRNA, *foxo* mutant adults, and in *Dp110$^{o/e}$, rpr* mutant adults (Figures 3I and 3K; Figure 4I; Figure S4A). In marked contrast, no neuroblasts were observed at these later time points in *RHG* miRNA-expressing adults or those mutant only for either *rpr* or *foxo* (Figures 3F, 3H, and 3K; data not shown). Thus, activation of the insulin/PI3 kinase pathway overcomes the caspase-independent mechanism that eliminates mb neuroblasts in *rpr* mutants and promotes long-term survival of mb neuroblasts in adult brains.

Does insulin/PI3 kinase activation suppress autophagy in persisting mb neuroblasts? Autophagic cell death as a result of downregulation of PI3 kinase signaling and apoptosis are both required for proper elimination of the *Drosophila* larval salivary gland [23]. To determine whether elimination of Foxo promotes long-term survival of *RHG* miRNA mb neuroblasts via inhibition of autophagy, we expressed a dominant-negative version of the autophagy-promoting protein ATG1 [24] in *RHG* miRNA mb neuroblasts. Again we observed Dpn-expressing mb neuroblasts in 1-month-old *ATG1 DN, RHG* miRNA animals, but not in animals expressing *ATG1 DN* alone in their neuroblasts (Figures 3J and 3K). Similar to *foxo* mutant animals, *ATG1 DN* mb neuroblasts also have a slight delay in their disappearance (data not shown). Therefore, downregulation of insulin/PI3 kinase may serve as a potent backup mechanism to ensure mb neuroblast elimination via activation of an autophagic cell death response.

Next we assayed the behavior of these long-term persisting adult mb neuroblasts. We observed that some, but not all, 2-week-old *RHG* miRNA, *foxo* mutant mb neuroblasts were large in size and generated many new progeny compared to young (3–5 days posteclosion) neuroblasts that either expressed *RHG* miRNA or were mutant for *rpr* (Figures 4A, 4C, 4D, 4F, and 4H). Similarly, some young (3–5 day posteclosion) *RHG* miRNA, *foxo* mb neuroblasts were also larger in size and generated many more progeny (Figures 4A, 4B, and 4E), suggesting that increased levels of nuclear Foxo also restrict proliferation and growth in mb neuroblasts inhibited for Reaper family proteins. Similar results were observed in *Dp110$^{o/e}$*, *rpr* mutant animals (Figure 4G; Figure S4B). Interestingly, we observed a strong correlation between mb neuroblast cell size and progeny number in 2-week-old *RHG* miRNA, *foxo* mutant adults, but not in younger mutant adults (Figures 4B and 4C). Thus, activation of the growth-promoting insulin/PI3 kinase pathway not only sustains long-term survival of adult mb neuroblasts but also increases their proliferation and growth rate. Furthermore, Foxo inactivation may indirectly allow long-term persisting adult mb neuroblasts to acquire growth properties common to neuroblasts during development.

Long-Term Surviving Adult Mushroom Body Neuroblasts Generate New mb Neurons

Finally, we analyzed the morphology of the newborn cells by visualizing mCD8:GFP, which perdures transiently in daughter cells following neuroblast cell divisions (Figures 4I and 4K). Dendrites appeared to project normally into the mb calyx (Figure 4J, arrow), whereas the trajectory of axons was more variable (Figure 4K). We observed bundles of axons that projected normally through the mb pedunculus (Figure 4K, right) and some that mistargeted, bifurcating prematurely and projecting anterior to the pedunculus (Figure 4K, left). Axon pathfinding defects could arise from limited guidance cues in the fully developed adult brain. Alternatively, some of these supernumerary neurons may have an inappropriately specified identity. We observed no defects in the mushroom body structure of *RHG* miRNA or *foxo* mutant adults. Thus, at least a subset of supernumerary mb neurons generated from long-term surviving mb neuroblasts appear to incorporate into the existing mature adult mushroom body structure.

Conclusions

Our findings demonstrate that two pathways act in concert to eliminate mb neuroblasts and terminate neurogenesis (Figure 4L). Downregulation of insulin/PI3 kinase signaling

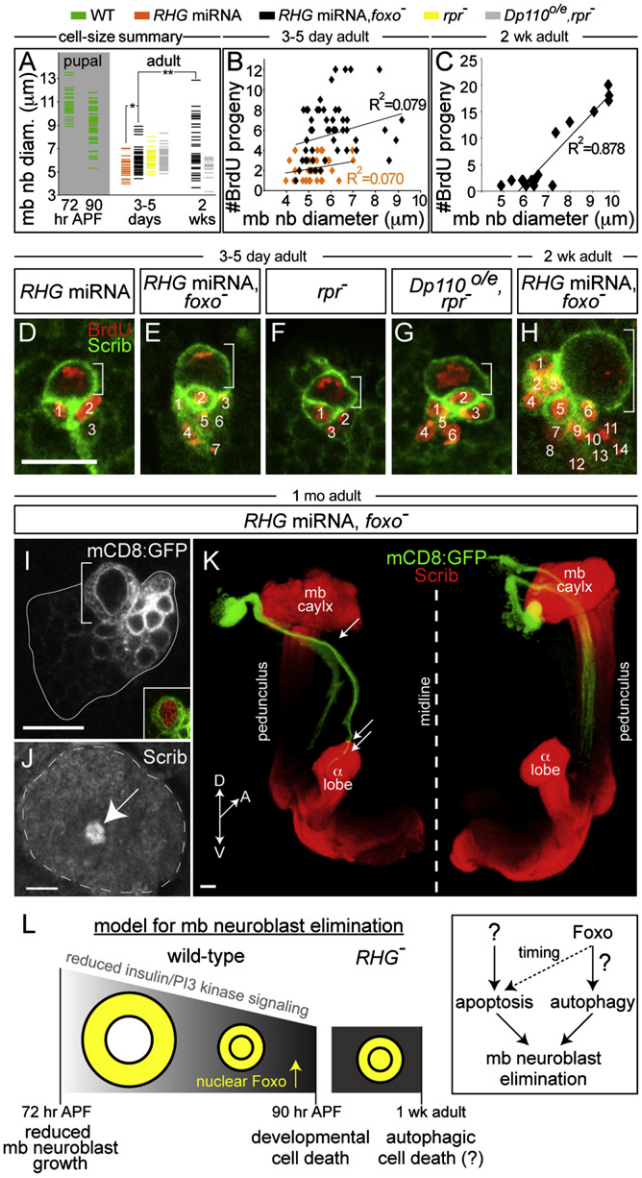

Figure 4. Long-Term Surviving mb Neuroblasts Proliferate and Generate New Adult mb Neurons

(A–C) Summary of mb neuroblast cell size over time. Genotypes are color-coded at top for (A)–(C). Each dash (A) or diamond (B and C) represents one neuroblast.

(A) *p < 0.003, **p < 0.0003.

(B and C) Number of BrdU progeny generated in 24 hr relative to mb neuroblast cell size. Foxo restricts mb neuroblast proliferation rate and cell size. mb neuroblast cell size and proliferation rate correlate in 2-week-old *RHG* miRNA, *foxo*$^{-}$ adults (C), but not in 3- to 5-day-old adults (B). R^2 denotes coefficient of determination for a linear correlation.

(D–H) mb neuroblasts (white brackets) and progeny (numbered) following a 24 hr BrdU treatment.

(H) Only 14 of 18 progeny are shown.

(I and K) 1-month-old adult mb neuroblasts (I, bracket) generate new mb neurons, cell bodies (I, outline), and axons (K). Inset is double-labeled neuroblast, mCD8:GFP (green) and Dpn (red). Genotype: *worniuGAL4*, *UASmCD8:GFP*, *UAS-RHG* miRNA, *foxo*$^{-}$/*foxo*$^{-}$ (K). Reconstruction of the mushroom body (red) with overlay of newborn adult neurons (mCD8:GFP, green) is shown.

(J) Dendrites from new neurons project normally to the mb calyx (arrow, 2-week-old adult).

occurs first and may activate both autophagy and a program of caspase-dependent cell death. In the absence of one of these cell death pathways, mb neuroblasts persist, but only transiently. Thus, a fail-safe mechanism likely exits to ensure mb neuroblast elimination, similar to salivary gland cells [23].

The reduction in growth that precedes neuroblast apoptosis appears to be developmentally regulated because it occurs at an earlier time in central brain neuroblasts than in mushroom body neuroblasts. This may be due to either local differences in microenvironments or differences in the ability of neuroblasts to respond to circulating insulin-like peptides [25]. Moreover, the extended survival of mb neuroblasts under these conditions, but not of other central brain neuroblasts, suggests that additional mechanisms such as terminal differentiation still function to ensure elimination of most neuroblasts [4, 26]. Indeed, during mammalian development, neural progenitors are eliminated via cell death and by terminal differentiation. The relative importance of death and differentiation for neuroblast elimination may be lineage dependent. Finally, because cricket adult mb neuroblasts proliferate in response to insulin in explant cultures [27], a common mechanism may regulate adult neurogenesis among insects and possibly in more distantly related metazoans. Our findings may represent an important first step toward devising ways to manipulate the regenerative capacity of adult brains in diverse species and provide insight into how aberrantly persisting neural stem cells behave in vivo.

Experimental Procedures

We used the following fly stocks: *w;FRT80B,Df(3L)H99*, *XR38*, *foxo*^{25}, *UAS-GFP,tub-GAL4;FRT80B,tub-GAL80*, *worniu-GAL4* [12], *UAS-p35*, *UAS-flp*, *hsp70flp;act5c-FRT-stop-FRT-tau:lacZ*, *tub-GAL80[ts]*, *UAS-mCD8:GFP*, *UAS-Dp60*, *UAS-InRCA* (BL#8263), *UAS-Dp110*, *UAS-InRDN* (BL#8252), *UAS-ATG1DN (UAS-ATG1*^{K38Q}*)*, *pcnaeGFP*, and OregonR. We replaced eGFP with GAL4 in the pRD119 transformation vector [14] to generate *pcna-GAL4*. We used the miRNA mir6.1 method [28] to generate *UAS-RHG* miRNA. *rpr*, *hid*, and *grim* sequences (Figure S2) were subcloned into one of three stem-loop units and ligated into pUAST or pGMR. Transgenic animals were generated by BestGene.

Neuroblast clones were induced by shifting freshly eclosed adults (*pcnaGAL4*, *UASflp*, *tubGAL80[ts]*, *act5c-FRT-stop-FRT-tauLacZ*;Df(3L)H99/Df(3L)XR38) to 30°C or to 37°C for 15 min (hsflp;act > stop > tauLacZ; H99/XR28). MARCM animals were shifted to 37°C for 1 hr at white pupal stages. Adults were fed BrdU (0.5 mg/ml) mixed with yeast paste and food dye for 24 or 48 hr.

Adult and pupal brains were fixed for 25 min in 4% paraformaldehyde/PEM buffer (Pipes, EGTA, $MgCl_2$) and processed with standard methods [12]. White pupae were picked (t = 0 hr) and aged accordingly. We used Lamin (Developmental Studies Hybridoma Bank, #ADL67.10) and other antibodies previously described [12, 20]. For BrdU labeling, brains were incubated in 2 N HCl for 30 min before processing. Cell death was assayed with a TUNEL kit (Roche). Labeling reaction proceeded for 1 hr at 37°C. All images were collected on a confocal microscope, and images were processed with ImageJ, Adobe Photoshop, and Adobe Illustrator software.

Brains were imaged from the ventral to dorsal surface. When neuroblasts were too small to be distinguished by size, we counted only isolated Dpn-expressing cells. The small Dpn-expressing cells generated from intermediate progenitors that reside mostly in clusters on the dorsal brain surface were not counted. Average neuroblast diameter was determined by

(K) Axons either project normally through the mb pedunculus (right) or mistarget (left). Single arrow marks premature axon bifurcation (left), and double arrow marks termination at the top of the α lobe.

(L) A model for the mechanism by which mb neuroblasts are eliminated (see Results and Discussion). *worniuGAL4* is used to induce UAS transgene expression (A–E and G–K).

Scale bars in (D) and (I)–(K) equal 10 μm. See also Figure S4.

measuring the length of two perpendicular lines, each passing through the neuroblast center. Average pixel intensity was determined for three separate equal-sized regions in the cytoplasm and in the nucleus and was then averaged. Student's two-tailed t test was performed for statistical significance.

Supplemental Information

Supplemental Information includes four figures and two movies and can be found with this article online at doi:10.1016/j.cub.2010.01.060.

Acknowledgments

We thank E. Baehrecke, C. Doe, B. Duriano, M. Freeman, K. White, B. Edgar, R. Tjian, the Bloomington Stock Center, the Developmental Studies Hybridoma Bank, and the *Drosophila* Genomics Resource Center for fly stocks, antibodies, and/or constructs. We thank K. Siller, N. Patel, D. Bilder, A. Gerhold, C. Doe, D. Weisblat, and J. Boone for discussions and/or reading of the manuscript. S.E.S. is a Robert Black Fellow of the Damon Runyon Cancer Research Foundation (DRG-1960-07), and I.K.H. is funded by the National Institutes of Health (RO1 GM61672, RO1 GM85576).

Received: November 17, 2009
Revised: January 20, 2010
Accepted: January 29, 2010
Published online: March 25, 2010

References

1. Dufour, M.C., and Gadenne, C. (2006). Adult neurogenesis in a moth brain. J. Comp. Neurol. *495*, 635–643.
2. Zhao, X., Coptis, V., and Farris, S.M. (2008). Metamorphosis and adult development of the mushroom bodies of the red flour beetle, Tribolium castaneum. Dev. Neurobiol. *68*, 1487–1502.
3. Cayre, M., Scotto-Lomassese, S., Malaterre, J., Strambi, C., and Strambi, A. (2007). Understanding the regulation and function of adult neurogenesis: Contribution from an insect model, the house cricket. Chem. Senses *32*, 385–395.
4. Maurange, C., Cheng, L., and Gould, A.P. (2008). Temporal transcription factors and their targets schedule the end of neural proliferation in Drosophila. Cell *133*, 891–902.
5. von Trotha, J.W., Egger, B., and Brand, A.H. (2009). Cell proliferation in the Drosophila adult brain revealed by clonal analysis and bromodeoxyuridine labelling. Neural Dev *4*, 9.
6. Ito, K., and Hotta, Y. (1992). Proliferation pattern of postembryonic neuroblasts in the brain of Drosophila melanogaster. Dev. Biol. *149*, 134–148.
7. Kato, K., Awasaki, T., and Ito, K. (2009). Neuronal programmed cell death induces glial cell division in the adult Drosophila brain. Development *136*, 51–59.
8. Knoblich, J.A. (2008). Mechanisms of asymmetric stem cell division. Cell *132*, 583–597.
9. Doe, C.Q. (2008). Neural stem cells: Balancing self-renewal with differentiation. Development *135*, 1575–1587.
10. Zhong, W., and Chia, W. (2008). Neurogenesis and asymmetric cell division. Curr. Opin. Neurobiol. *18*, 4–11.
11. Truman, J.W., and Bate, M. (1988). Spatial and temporal patterns of neurogenesis in the central nervous system of Drosophila melanogaster. Dev. Biol. *125*, 145–157.
12. Lee, C.Y., Robinson, K.J., and Doe, C.Q. (2006). Lgl, Pins and aPKC regulate neuroblast self-renewal versus differentiation. Nature *439*, 594–598.
13. Lee, T., and Luo, L. (1999). Mosaic analysis with a repressible cell marker for studies of gene function in neuronal morphogenesis. Neuron *22*, 451–461.
14. Thacker, S.A., Bonnette, P.C., and Duronio, R.J. (2003). The contribution of E2F-regulated transcription to Drosophila PCNA gene function. Curr. Biol. *13*, 53–58.
15. Kurusu, M., Maruyama, Y., Adachi, Y., Okabe, M., Suzuki, E., and Furukubo-Tokunaga, K. (2009). A conserved nuclear receptor, Tailless, is required for efficient proliferation and prolonged maintenance of mushroom body progenitors in the Drosophila brain. Dev. Biol. *326*, 224–236.
16. Bello, B.C., Hirth, F., and Gould, A.P. (2003). A pulse of the Drosophila Hox protein Abdominal-A schedules the end of neural proliferation via neuroblast apoptosis. Neuron *37*, 209–219.
17. Peterson, C., Carney, G.E., Taylor, B.J., and White, K. (2002). reaper is required for neuroblast apoptosis during Drosophila development. Development *129*, 1467–1476.
18. Hay, B.A., and Guo, M. (2006). Caspase-dependent cell death in Drosophila. Annu. Rev. Cell Dev. Biol. *22*, 623–650.
19. Jünger, M.A., Rintelen, F., Stocker, H., Wasserman, J.D., Végh, M., Radimerski, T., Greenberg, M.E., and Hafen, E. (2003). The Drosophila forkhead transcription factor FOXO mediates the reduction in cell number associated with reduced insulin signaling. J. Biol. *2*, 20.
20. Puig, O., Marr, M.T., Ruhf, M.L., and Tjian, R. (2003). Control of cell number by Drosophila FOXO: Downstream and feedback regulation of the insulin receptor pathway. Genes Dev. *17*, 2006–2020.
21. Weinkove, D., Neufeld, T.P., Twardzik, T., Waterfield, M.D., and Leevers, S.J. (1999). Regulation of imaginal disc cell size, cell number and organ size by Drosophila class I(A) phosphoinositide 3-kinase and its adaptor. Curr. Biol. *9*, 1019–1029.
22. Leevers, S.J., Weinkove, D., MacDougall, L.K., Hafen, E., and Waterfield, M.D. (1996). The Drosophila phosphoinositide 3-kinase Dp110 promotes cell growth. EMBO J. *15*, 6584–6594.
23. Berry, D.L., and Baehrecke, E.H. (2007). Growth arrest and autophagy are required for salivary gland cell degradation in Drosophila. Cell *131*, 1137–1148.
24. Scott, R.C., Juhász, G., and Neufeld, T.P. (2007). Direct induction of autophagy by Atg1 inhibits cell growth and induces apoptotic cell death. Curr. Biol. *17*, 1–11.
25. Brogiolo, W., Stocker, H., Ikeya, T., Rintelen, F., Fernandez, R., and Hafen, E. (2001). An evolutionarily conserved function of the Drosophila insulin receptor and insulin-like peptides in growth control. Curr. Biol. *11*, 213–221.
26. Fichelson, P., Moch, C., Ivanovitch, K., Martin, C., Sidor, C.M., Lepesant, J.A., Bellaiche, Y., and Huynh, J.R. (2009). Live-imaging of single stem cells within their niche reveals that a U3snoRNP component segregates asymmetrically and is required for self-renewal in Drosophila. Nat. Cell Biol. *11*, 685–693.
27. Malaterre, J., Strambi, C., Aouane, A., Strambi, A., Rougon, G., and Cayre, M. (2003). Effect of hormones and growth factors on the proliferation of adult cricket neural progenitor cells in vitro. J. Neurobiol. *56*, 387–397.
28. Chen, C.H., Huang, H., Ward, C.M., Su, J.T., Schaeffer, L.V., Guo, M., and Hay, B.A. (2007). A synthetic maternal-effect selfish genetic element drives population replacement in Drosophila. Science *316*, 597–600.